

Constraining the ortho-to-para ratio of H₂ with anomalous H₂CO absorption^{*}

N. Troscompt, A. Faure, S. Maret, C. Ceccarelli, P. Hily-Blant, and L. Wiesenfeld

Laboratoire d'Astrophysique de Grenoble, Université Joseph Fourier, UMR 5571-CNRS, Grenoble, France
e-mail: Nicolas.troscompt@obs.ujf-grenoble.fr

Received 26 June 2009 / Accepted 5 August 2009

ABSTRACT

Context. The ortho-to-para ratio (OPR) of molecular hydrogen is a fundamental parameter in understanding the physics and chemistry of molecular clouds. In dark and cold regions, however, H₂ is not directly observable and the OPR of H₂ in these sources has so far remained elusive.

Aims. We show that the 6 cm absorption line of ortho-formaldehyde (H₂CO) can be employed to constrain both the density and the OPR of H₂ in dark clouds.

Methods. Green Bank Telescope (GBT) observations of ortho-H₂CO toward the molecular cloud Barnard 68 (B68) are reported. Non-LTE radiative transfer calculations combined with the well-constrained structure of B68 are then employed to derive the physical conditions in the absorption region.

Results. We provide the first firm confirmation of the Townes & Cheung mechanism: propensity rules for the collisions of H₂CO with H₂ molecules are responsible for the sub-2.7 K cooling of the 6 cm doublet. Non-LTE calculations show that in the absorption region of B68, the kinetic temperature is ~10 K, the ortho-H₂CO column density amounts to ~2.2 × 10¹³ cm⁻², the H₂ density is in the range 1.4–2.4 × 10⁴ cm⁻³, and the OPR of H₂ is close to zero. Our observations thus provide fresh evidence that H₂ is mostly in its para form in the cold gas, as expected from theoretical considerations. Our results also suggest that formaldehyde absorption originates in the edge of B68, at visual extinctions $A_V \lesssim 0.5$ mag.

Key words. astrochemistry – ISM: molecules – ISM: abundances – ISM: individual objects: Barnard 68

1. Introduction

The ortho-to-para ratio (OPR) of molecular hydrogen (H₂) is a fundamental parameter in understanding the physics and chemistry of interstellar molecular clouds. Chemical models have shown, in particular, that the degree of deuteration of molecular ions and molecules during the pre-protostellar collapse is very sensitive to the form of H₂ (Flower et al. 2006; Pagani et al. 2009). In these environments, H₂ forms on grain surfaces, and it is generally assumed that the initial OPR is equal to the statistical value of 3. Although the details of the H₂ formation mechanism remain uncertain, it is also commonly accepted that ortho-to-para conversion of H₂ occurs subsequently in the gas phase by means of proton exchange reactions with H⁺ and H₃⁺. Although the timescales associated with these reactions are large, the OPR of H₂ is expected to decrease toward zero (the Boltzmann equilibrium value at 10 K is 3.6 × 10⁻⁷) during the lifetime of a molecular cloud and it is, therefore, a potentially valuable probe of the age of the cloud. This ratio is however expected to be not fully thermalized in dark clouds because of the recycling of hydrogen via gas phase reactions and catalysis on grains (Le Bourlot 1991). The chemical modelling of Flower et al. (2006) for $n_H = 10^4$ cm⁻³ and $T = 10$ K thus suggests that the OPR is ~10⁻³ at steady-state, that is exceeds the Boltzmann equilibrium value by 4 orders of magnitude. In addition, in the

warm gas associated with molecular shocks ($T_{\text{kin}} > 300$ K), direct observations of H₂ rovibrational lines have shown that the OPR is generally not equal to the Boltzmann equilibrium value of 3, but lies in the range 0.5–2 (e.g., Neufeld et al. 1998; Lefloch et al. 2003; Maret et al. 2009, and references therein). These relatively low values are interpreted as the legacy of earlier stages of the thermal history of the gas. There is therefore evidence, both observational and theoretical, that H₂ is mostly in its para form in cold and dark progenitor molecular clouds. However, since the gas temperature in this latter type of clouds is too low to populate excited levels of H₂, a direct measure of the OPR of cold H₂ has remained so far elusive.

The OPR of H₂ is also important for collisional excitation processes at low temperature because the interaction potential is different for ground state para-H₂ ($J = 0$) and ortho-H₂ ($J = 1$). This is because the permanent quadrupole moment of H₂ vanishes when H₂ is in its spherically symmetric ground para state ($J = 0$). As a result, rate coefficients with ortho-H₂ ($J = 1$) are generally higher than those with para-H₂ ($J = 0$). Collisional propensity rules can also be different for the two forms of H₂, as shown for example by Flower et al. (1990) in the case of ammonia and, more recently, by Troscompt et al. (2009) in the case of formaldehyde (H₂CO). One particularly interesting observation of (ortho) H₂CO is the absorption of the 6 cm line ($1_{10} \leftarrow 1_{11}$) against the 2.7 K Cosmic Microwave Background (CMB). This “anomalous” absorption, which implies an excitation temperature $T_{\text{ex}} < 2.7$ K for the doublet, was first discovered by Palmer et al. (1969) in the direction of dark nebulae. Numerous

^{*} This work has been inspired by our colleague and friend Pierre Valiron, who passed away in August 2008. This paper is dedicated to his memory.

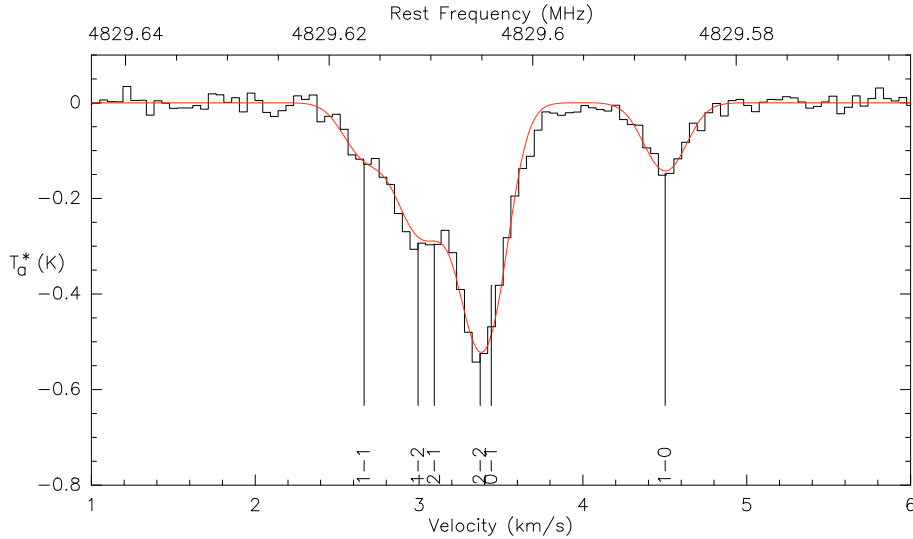


Fig. 1. Spectrum of the $1_{10} \leftarrow 1_{11}$ absorption line of ortho-H₂CO at 4.82966 GHz toward B68. The GBT spectrum is given by the black line while the red line denotes the CLASS HFS fit. The hyperfine transitions $1_{10} F' \leftarrow 1_{11} F$ are marked at their respective frequencies.

theoretical studies (in particular Townes & Cheung 1969; Evans et al. 1975; Garrison et al. 1976) proposed an explanation in terms of competing radiative and collisional population transfer mechanisms. The H₂CO absorption was thus found to provide a sensitive probe of the temperature and density conditions in dark sources. All previous studies were however hampered by i) the lack of accurate collisional rates between H₂CO and H₂ (He atoms were employed as substitutes for H₂ molecules) and ii) low spectral resolution, which did not allow to properly resolve the hyperfine structure.

In this study, we present the first high spectral resolution observation of the H₂CO 6 cm absorption line toward Barnard 68 (hereafter B68), the prototype of a dense molecular cloud (Burkert & Alves 2009, and references therein). Non-local thermodynamic equilibrium (LTE) radiative transfer calculations based on the theoretical collisional rates of Troscompt et al. (2009) are then employed to derive the physical conditions in the absorption region, including constraints on the OPR of H₂ in this source. The observations and data reduction are described in Sect. 2. Radiative transfer modelling is presented in Sect. 3, and results are discussed in Sect. 4.

2. Observations

We observed the $1_{10} \leftarrow 1_{11}$ transition of ortho-H₂CO ($\nu = 4.82966$ GHz) towards B68 (RA = 17^h22^m38.2^s, $\delta = -23^{\circ}49'34''$ [J2000]) using the NRAO Robert C. Byrd Green Bank Telescope (GBT). The observation was performed on October 17, 2008. The C-band (3.95–6.1 GHz) receiver was used together with the GBT auto-correlator in nine-level sampling mode, providing a spectral resolution of 762.9 Hz (0.047 km s⁻¹). At the observed frequency, the HPBW of the GBT is 2.5' and the main beam efficiency is $\eta_{\text{mb}} = 0.97$. The observations were performed in frequency switching mode, with a frequency throw of 100 MHz. Finally, the observation is an average of 4×10 min scans, for a total integration time of 40 min.

The data was reduced with the CLASS software package¹. A first order polynomial baseline was subtracted from the spectrum, which is shown in Fig. 1. Because of the high resolution

and high signal-to-noise ratio of the spectrum, several hyperfine components are resolved. Especially, the $F = 1-1$ and the (blended) $F = 1-2$ and $2-1$ components are clearly distinguishable from the (blended) $F = 2-2$ and $0-1$ components. The $F = 1-0$ component is also easily resolved. The line parameters were fitted with the HFS method in CLASS, which allows the simultaneous fitting of all the hyperfine components of a rotational transition, based on the assumption that the excitation temperature is the same for all hyperfine components and the lines do not overlap. We note that the frequencies and relative intensities of hyperfine components were taken from the laboratory measurements of Tucker et al. (1971). As shown in Fig. 1, an excellent fit to the observed spectrum is obtained, with a rms of $\sim 10^{-2}$ K.

We derived an antenna temperature T_a^* of the main hyperfine component ($F = 2-2$) of -0.44 ± 0.04 K, a source velocity $v_{\text{LSR}} = 3.374 \pm 0.003$ km s⁻¹, a total opacity of the transition $\tau_{\text{tot}} = 1.29 \pm 0.19$, and a line width $\Delta v = 0.294 \pm 0.007$ km s⁻¹. The excitation temperature was then derived from T_a^* within the Rayleigh-Jeans approximation (e.g., Martin & Barrett 1978) by assuming no clumping, that is a beam dilution factor of 1 since the spatial extent of B68 (2') and the beam extension (2.5') are similar. We obtained $T_{\text{ex}} = 1.63^{+0.19}_{-0.25}$ K. The present excitation temperature and opacity are thus in good agreement with those obtained by Heiles (1973), who found an average excitation temperature of 1.6 K and total opacities of ~ 1 for a sample of dark clouds.

3. Non-LTE modelling

The collisional pumping mechanism invoked to explain the anomalous absorption of H₂CO was first proposed by Townes & Cheung (1969). It was based on a classical formulation showing that collisions with neutral particles should favor excitation to the lower level of each doublet of ortho-H₂CO. This collisional propensity rule, combined with the dipolar radiative selection rules, leads to an overpopulation of the 1_{11} level and a cooling of the excitation temperature of the $1_{10} \leftarrow 1_{11}$ transition below 2.7 K². This scheme was subsequently supported by semi-classical and quantum calculations (Garrison et al. 1976).

² This phenomenon is also observed for the $2_{11} \leftarrow 2_{12}$ transition of ortho-H₂CO at 2 cm.

¹ GILDAS package, <http://www.iram.fr/IRAMFR/GILDAS>

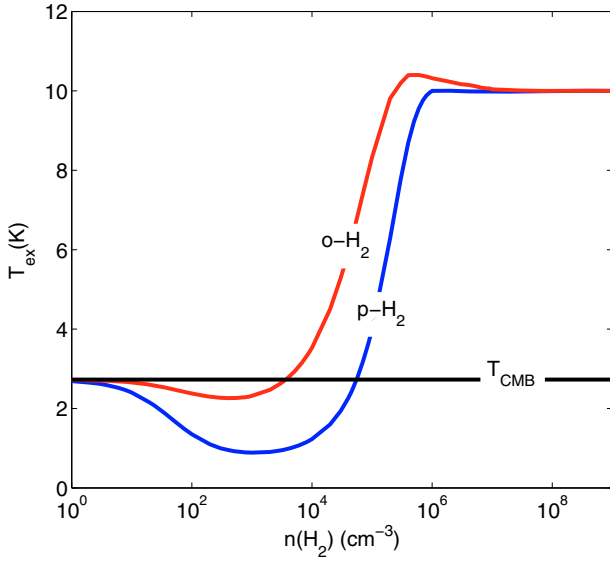


Fig. 2. Excitation temperature for the $1_{10} \leftarrow 1_{11}$ transition as a function of the H₂ density. The blue and red lines correspond to para-H₂ ($J = 0$) and ortho-H₂ ($J = 1$) as collider, respectively. The black horizontal solid line denotes the background temperature $T_{\text{CMB}} = 2.7$ K. See text for details.

However, as mentioned in the introduction, He atoms were employed as substitutes for H₂ in all previous studies. Troscompt et al. (2009) showed that the propensity rule is weaker for H₂ than for He and, furthermore, that it depends significantly on the ortho/para form of H₂.

This is clearly illustrated in Fig. 2, where we plot the results of a non-LTE computation based on collisional excitation by either para-H₂ ($J = 0$) and He atoms or ortho-H₂ ($J = 1$) and He atoms. We note, however, that excitation by H₂ is entirely predominant, that is the contribution of He atoms was found to be negligible. Excitation by the far less abundant free electrons was neglected³. The hyperfine structure of H₂CO levels was neglected in the calculations (see below). We employed the MOLPOP program, written by Moshe Elitzur and Philip Lockett, to solve the radiative transfer equations using the escape probability method for a homogeneous slab (Krolik & McKee 1978). The 10 first levels of ortho-H₂CO were considered in the computation with the following basic parameters: the ortho-H₂CO column density was fixed to $N(\text{H}_2\text{CO}) = 1.0 \times 10^{13} \text{ cm}^{-2}$, the kinetic temperature to $T_{\text{kin}} = 10$ K, and the Doppler linewidth to 1 km s^{-1} . The 2.7 K CMB radiation field was obviously included but all other possible sources of radiation were neglected. The collisional data was those of Troscompt et al. (2009) and Green (1991) for excitation by H₂ and He, respectively. It is first observed, in agreement with previous calculations based on He as a collider, that cooling of the 6 cm doublet below 2.7 K does occur for densities lower than a few 10^4 cm^{-3} . This provides the first robust confirmation of the Townes & Cheung mechanism in the case of H₂ as a collider. Secondly, it is noticed that the cooling is significantly stronger for para-H₂ ($J = 0$) than for ortho-H₂ ($J = 1$), and that it occurs over a wider range of density. Hence, the cooling of the doublet is expected to depend markedly on the OPR of H₂, with diminishing intensity of the 6 cm absorption line as the OPR increases.

³ We note that electron excitation of H₂CO can play an important role at high electron fraction ($x_e \gtrsim 10^{-5}$), in particular in diffuse clouds where electron collisions are expected to cancel the anomalous 6 cm absorption (Turner 1993).

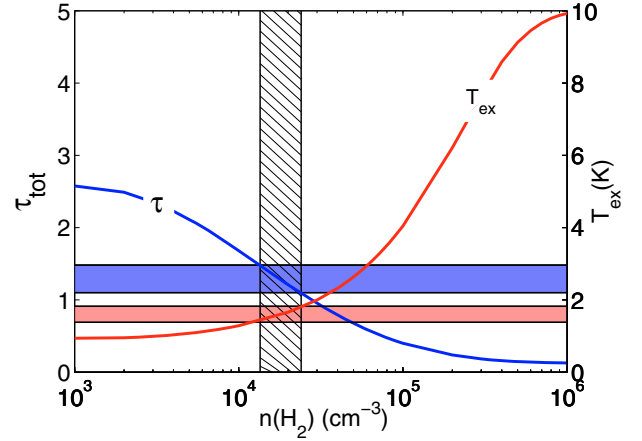


Fig. 3. Total opacity, τ_{tot} , and excitation temperature, T_{ex} , as a function of density. The blue and red shaded area denote respectively the range of observed τ_{tot} and T_{ex} . The blue and red lines denote the results of the present model for a kinetic temperature of 10 K, an ortho-H₂CO column density of $2.2 \times 10^{13} \text{ cm}^{-2}$ and an OPR of H₂ of zero. The dashed area indicates the density range where both τ_{tot} and T_{ex} are reproduced.

As mentioned above, we neglected the hyperfine splitting of the H₂CO transitions in our radiative transfer treatment. This approximation is strictly valid only when the separation of the hyperfine lines is negligible compared to the line broadening. For linear molecules with large splittings, e.g., HCN or N₂H⁺, detailed treatments have shown that the total opacity of rotational lines can be uncertain by up to a factor of two (for $\tau_{\text{tot}} \gg 1$) if the hyperfine structure is neglected (Daniel et al. 2006). In the case of H₂CO, accurate hyperfine collisional rates are not available because the two-spin recoupling formalism (see Daniel et al. 2004) has not yet been extended to asymmetric tops. However, we assessed the effect of the hyperfine structure by resorting to the approximation that hyperfine rates are proportional to the degeneracy ($2F' + 1$) of the final hyperfine level. Ad hoc selection rules such as $\Delta F = 0$ were also tested at both low and high opacities ($0 < \tau_{\text{tot}} < 50$). Line overlap was included using the absorption probability method (Lockett & Elitzur 1989). The total opacity and excitation temperature (common to all hyperfine levels) were found to agree to within 10% with calculations considering only the rotational structure. As a result, in contrast to molecules containing a ¹⁴N nucleus, the hyperfine structure in H₂CO can safely be neglected.

Based on the previous considerations, grids of models were constructed by varying the H₂ density between 10^3 and 10^6 cm^{-3} and the kinetic temperature between 7 and 12 K, in accordance with the known physical structure of B68 (Bergin et al. 2006); the ortho-H₂CO column density was varied between 10^{11} and 10^{15} cm^{-2} , and the OPR of H₂ between 0 and 3, with the objective of reproducing both the total opacity τ_{tot} and the excitation temperature T_{ex} reported in Sect. 2. The line width was fixed at 0.294 km s^{-1} , as deduced from the CLASS HFS fit. It should be noted that the impact of temperature variation (7–12 K) was found to be negligible in our modelling. In the following, we therefore assume a constant temperature of 10 K. On the other hand, the ortho-H₂CO column density was found to be very well constrained by our observations, with a value of $2.2 \pm 0.8 \times 10^{13} \text{ cm}^{-2}$. Interestingly, both the excitation temperature and line total opacity were found to depend strongly on the assumed H₂ density and OPR. This is illustrated in Fig. 3, which shows the predicted opacity and excitation temperature as a function of the H₂ density, assuming an OPR equal to zero. In

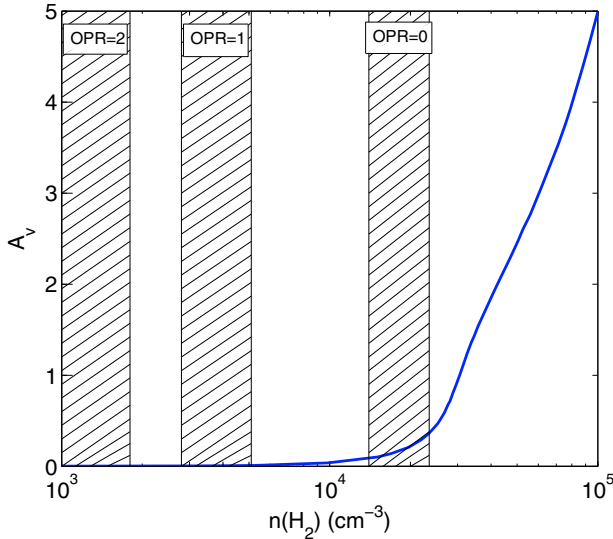


Fig. 4. Visual extinction A_v in B68 as a function of H₂ density adopted from the model of Alves et al. (2001). The dashed areas denote the ranges of H₂ densities compatible with our H₂CO observation for OPR equal to 0, 1, and 2, respectively.

this particular case, our observations constrain the H₂ density to the narrow range $1.4 \times 10^4 - 2.4 \times 10^4 \text{ cm}^{-3}$.

For a higher OPR, the observed τ_{tot} and T_{ex} can still be reproduced simultaneously but for much lower H₂ densities. This is shown in Fig. 4, where we plot the allowed range of densities for an OPR of 0, 1, and 2 respectively. It should be noted that the dependence of our model on the OPR is linear and not logarithmic. As a result, we can obviously not discriminate between an OPR of zero and, e.g., 10^{-3} . We also report in Fig. 4 the visual extinction of B68 as a function of density, as derived by Alves et al. (2001). The case OPR = 3 is not plotted because it is not compatible with the observations. This figure shows that the H₂ densities compatible with our H₂CO observation relate to the low visual extinction, $A_v \lesssim 0.5$ mag, that is in the outer parts of the core. In the following paragraph, we discuss the implications of this result.

4. Discussion

Our observations and modelling have demonstrated that the H₂CO abnormal absorption originates in regions of the core of moderate extinction. However, the precise origin of the absorption depends on the H₂ OPR. Conversely, one can place constraints on the OPR from simple arguments about the chemistry of the molecule. In particular, it is unlikely that the absorption of H₂CO occurs in regions where $A_v < 0.1$ mag. In these regions, the external UV field dissociates molecules and forms a photon-dominated layer. For example, in their detail modelling of the photon-dominated region (PDR) surface layer of B68, Pineda & Bensch (2007) found that the CO abundance peaks at higher visual extinctions ($A_v \sim 0.4$ mag). Although Pineda & Bensch do not present predictions for H₂CO, we expect its abundance to peak at a similar or slightly greater A_v because, unlike CO, H₂CO should not be self-shielded from the UV field. Deeper inside the cloud, the abundance of both molecules are expected to decrease, because of the freeze-out on grain mantles (e.g., Bergin et al. 2002; Maret & Bergin 2007, in the case of B68). If we assume that the observed H₂CO originates in a region where $A_v \sim 0.4$ mag, our modelling indicates that the OPR is close to 0 (see Fig. 4). As mentioned above, it is very unlikely

that the absorption originates in a region where $A_v < 0.1$ mag, and therefore the OPR is necessarily smaller than 1. Thus, our modelling and observations are consistent with $0 \leq \text{OPR} \lesssim 1$, that is with H₂ mostly in para form.

Furthermore, we have shown that the absorption originates in regions where $A_v \lesssim 0.5$ mag, that is the ortho-H₂CO 6 cm absorption line probes the outermost envelope of B68. This conclusion was first reached by Minn & Greenberg (1975). Additional evidence supporting this scenario was subsequently obtained by Henkel et al. (1981) for TMC-1 and by Vanden Bout et al. (1983) for a sample of seven dark clouds. It is interesting to note that our estimate of the ortho-H₂CO column density in B68 ($2.2 \pm 0.8 \times 10^{13} \text{ cm}^{-2}$) is consistent with the range obtained by the previous authors ($10^{12} - 10^{14} \text{ cm}^{-2}$). Assuming $A_v = 0.4$ mag and using the relation $N(\text{H}_2)/A_v = 0.94 \times 10^{21} \text{ cm}^{-2} \text{ mag}^{-1}$ (Frerking et al. 1982), we obtained an H₂CO relative abundance (in the absorption region) of $X(\text{H}_2\text{CO}) \sim 6 \times 10^{-8}$. In the envelope of dark clouds, such a large abundance cannot be reproduced by gas phase chemistry models, as first pointed out by Federman & Allen (1991). In the gas phase, H₂CO is mainly formed by the reaction of atomic oxygen with CH₃. However, there is never enough CH₃ in the tenuous envelopes of dark clouds and, in addition, H₂CO is rapidly destroyed by photodissociation and by reactions with C⁺ (Federman & Allen 1991). Alternatively, H₂CO may form by successive hydrogenation of CO at the surface of the grains (Tielens & Hagen 1982). This mechanism is expected to be more efficient in the innermost regions of the cores, where the depletion of CO is at its highest. Thus, this scenario would require an efficient mixing mechanism to bring the grains from the interior to the surface, where CO and H₂CO could be photo-evaporated. However, turbulence is observed to be small in B68 with both C¹⁸O and ¹³CO line widths being close to the thermal line width (Lada et al. 2003). Complex radial motions have been observed in this source, but their amplitude is also small ($< 0.05 \text{ km s}^{-1}$, Maret et al. 2007). As a result, we are currently unable to distinguish between gas phase and grain surface chemistry for the H₂CO formation, which has long been enigmatic in a variety of objects (e.g., Roueff et al. 2006). Future studies will address this important issue further. It will be interesting, in particular, to model other observable H₂CO lines, in particular the 2 mm emission ($2_{11} \rightarrow 1_{11}$) and 2 cm absorption ($2_{11} \leftarrow 2_{12}$). These two lines are, however, understood to originate in higher density regions than the 6 cm line (Vanden Bout et al. 1983). Interferometric observations would also clearly be desirable to probe the spatial distribution of H₂CO absorption in B68. We note that such observations were undertaken by Zhou et al. (1990) in a VLA study of the Bok globule B335.

It is finally interesting to compare the OPR that we derive in B68 to other estimates. Based on observations and modelling of the DCO⁺ and HCO⁺ emission in this source, Maret & Bergin (2007) inferred an OPR of 0.015, a value that is consistent with the value obtained here. Furthermore, Pagani et al. (2009) used N₂D⁺, N₂H⁺ and ortho-H₂D⁺ observations to derive the OPR in the L183 prestellar core, and found that it is 0.1 in most parts of the cloud. Finally, Maret et al. (2009) recently obtained maps of the H₂ OPR in the shocked gas in NGC 1333 cloud, from which they concluded that the OPR in cold, pre-shock gas is lower than 1. Thus, all these studies are consistent with the result presented here, that is H₂ is mostly in para form in cold gas.

Acknowledgements. Part of this work is funded by the french national program “Physico-Chimie du Milieu Interstellaire” (PCMI). Michel Guélin is acknowledged for fruitful suggestions. We specially thank Jim Braatz and all the staff of the Green Bank Telescope for all the valuable help they provided for a very successful observation.

References

- Alves, J. F., Lada, C. J., & Lada, E. A. 2001, *Nature*, 409, 159
- Bergin, E. A., Alves, J., Huard, T., & Lada, C. J. 2002, *ApJ*, 570, L101
- Bergin, E. A., Maret, S., van der Tak, F. F. S., et al. 2006, *ApJ*, 645, 369
- Burkert, A., & Alves, J. 2009, *ApJ*, 695, 1308
- Daniel, F., Dubernet, M.-L., & Meuwly, M. 2004, *J. Chem. Phys.*, 121, 4540
- Daniel, F., Cernicharo, J., & Dubernet, M.-L. 2006, *ApJ*, 648, 461
- Evans II, N. J., Morris, G., Sato, T., & Zuckerman, B. 1975, *ApJ*, 196, 433
- Federman, S. R., & Allen, M. 1991, *ApJ*, 375, 157
- Flower, D. R., Offer, A., & Schilke, P. 1990, *MNRAS*, 244, 4P
- Flower, D. R., Pineau Des Forêts, G., & Walmsley, C. M. 2006, *A&A*, 449, 621
- Frerking, M. A., Langer, W. D., & Wilson, R. W. 1982, *ApJ*, 262, 590
- Garrison, B. J., Lester Jr., W. A., & Miller, W. H. 1976, *J. Chem. Phys.*, 65, 2193
- Green, S. 1991, *ApJS*, 76, 979
- Heiles, C. 1973, *ApJ*, 183, 441
- Henkel, C., Wilson, T. L., & Pankonin, V. 1981, *A&A*, 99, 270
- Krolik, J. H., & McKee, C. F. 1978, *ApJS*, 37, 459
- Lada, C. J., Bergin, E. A., Alves, J. F., & Huard, T. L. 2003, *ApJ*, 586, 286
- Le Bourlot, J. 1991, *A&A*, 242, 235
- Lefloch, B., Cernicharo, J., Cabrit, S., et al. 2003, *ApJ*, 590, L41
- Lockett, P., & Elitzur, M. 1989, *ApJ*, 344, 525
- Maret, S., & Bergin, E. A. 2007, *ApJ*, 664, 956
- Maret, S., Bergin, E. A., & Lada, C. J. 2007, *ApJ*, 670, L25
- Maret, S., Bergin, E. A., Neufeld, D. A., et al. 2009, *ApJ*, 698, 1244
- Martin, R. N., & Barrett, A. H. 1978, *ApJS*, 36, 1
- Minn, Y. K., & Greenberg, J. M. 1975, *A&A*, 38, 81
- Neufeld, D. A., Melnick, G. J., & Harwit, M. 1998, *ApJ*, 506, L75
- Pagani, L., Vastel, C., Hugo, E., et al. 2009, *A&A*, 494, 623
- Palmer, P., Zuckerman, B., Buhl, D., & Snyder, L. E. 1969, *ApJ*, 156, L147
- Pineda, J. L., & Bensch, F. 2007, *A&A*, 470, 615
- Roueff, E., Dartois, E., Geballe, T. R., & Gerin, M. 2006, *A&A*, 447, 963
- Tielens, A. G. G. M., & Hagen, W. 1982, *A&A*, 114, 245
- Townes, C. H., & Cheung, A. C. 1969, *ApJ*, 157, L103
- Troscompt, N., Faure, A., Wiesenfeld, L., Ceccarelli, C., & Valiron, P. 2009, *A&A*, 493, 687
- Tucker, K. D., Tomasevich, G. R., & Thaddeus, P. 1971, *ApJ*, 169, 429
- Turner, B. E. 1993, *ApJ*, 410, 140
- Vanden Bout, P. A., Snell, R. L., & Wilson, T. L. 1983, *A&A*, 118, 337
- Zhou, S., Evans, II, N. J., Butner, H. M., et al. 1990, *ApJ*, 363, 168